Journal of Sol-Gel Science and Technology
https://doi.org/10.1007/s10971-020-05305-z

ORIGINAL PAPER: NANO-STRUCTURED MATERIALS (PARTICLES, FIBERS, COLLOIDS, COMPOSITES, ETC.)

# Optimization and evaluation of encapsulated brimonidine tartrate-loaded nanoparticles incorporation in situ gel for efficient intraocular pressure reduction

Pankaj Kumar Sharma[1] · Meenakshi Kanwar Chauhan[1]

Received: 26 January 2020 / Accepted: 28 April 2020


## Abstract

Brimonidine tartrate (BRT) is a water-soluble anti-glaucoma drug that is available in ophthalmic solution (Alphagan Z®). Various ocular barriers prevent permeation and precorneal retention of the drugs within the corneal region. In this study, BRT encapsulated vitamin E-tocopheryl polyethylene glycol succinate (TPGS)-polycaprolactone (PCL) nanoparticles were prepared to improve permeation through different physiological barriers of eyes. Optimized formulation comprising of PCL (0.4% w/v) and vitamin E TPGS (0.5% w/v) was characterized. It was revealed that formulation exhibited 243.40 ± 5.21 nm, 0.103 ± 0.020, 78.87 ± 5.32% and +3.23 ± 0.01 mV of mean particle size, polydispersibility index (PDI), percentage entrapment efficiency (%EE), and zeta potential respectively. Furthermore, optimized BRT loaded nanoparticles were incorporated into a poloxamer based in situ system and was characterized. In vitro study confirmed that around 93.91 ± 3.12% was the highest recorded of cumulative drug release in simulated aqueous humor over 24 h. Optimized formulation upon in vivo ocular irritability and tolerability tests were found to be well tolerated with no signs of irritation. A significant difference in percentage of intraocular pressure (IOP) reduction between marketed eye drop and optimized nanoparticles based in situ gel was observed in the glaucoma induced rabbit model. These experimental data revealed that nanoparticles based thermosensitive in situ gel could be utilized to enhance corneal residence time and ensure consistent IOP reduction.

## Graphical Abstract

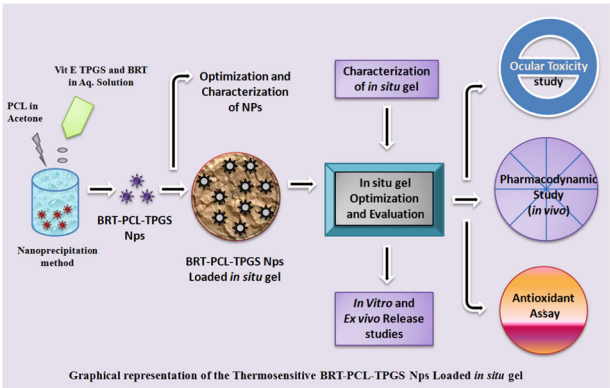


✉ Meenakshi Kanwar Chauhan
meenakshikanwar@yahoo.com

[1] Department of Pharmaceutics, NDDS Research Laboratory, Delhi Institute of Pharmaceutical Sciences and Research, DPSR-University, Pushp Vihar, Section 3, New Delhi 110017, India

Published online: 22 May 2020

**Keywords** Glaucoma · Brimonidine tartrate · Nanoparticles · Poloxamer 407 · In situ gel · Intraocular pressure study

**Highlights**

- PCL-TPGS nanoparticles of BRT were prepared using nanoprecipitation method.
- Drug nanoparticles were incorporated into thermosensitive in situ gel systems which provide sustained release than commercial eye drops.
- Optimized gels are non-irritating confirmed by ocular tolerance in vivo study.
- Developed Nano-gel exhibit IOP lowering capacity confirmed by animal model of glaucoma.

## 1 Introduction

The development of ocular drug delivery systems are the most preferred delivery system, attracting great interest due to its various expedient properties like non-invasiveness and for better control of glaucoma [1]. Approximately, 90% of ophthalmic dosage forms are available in form of ocular drops. Main disadvantage of the eye drop is drug loss if washed out from surface of the eye due to short precorneal contact time and lower corneal permeability that results in less bioavailability contact time with the cornea and therefore, frequently administration of dosage is needed to achieve a therapeutic action during the treatment [2]. Based on the literature data, various ocular drug delivery systems including nanoemulsion [3], liposomes [4], niosomes [5], microparticles [6] has been explored and tested to improve precorneal residence time and drug permeation through the cornea. These delivery systems are fabricated by the FDA approved natural and synthesized polymers like eudragit [7], hyaluronate [8], cyclodextrins [9], polylactic acid (PLA) [10], chitosan [11], poly (vinyl alcohol) [12], poly (vinyl-pyrrolidone) [13], poly(lactic acid-co-glycolic acid) PLGA, and PCL [14], etc. for ocular route. However, long term storage stability and their fast clearance associated with above mentioned ocular drug delivery systems have been proved. To overcome these problems, another approach for the improvement of efficacy of drug by improving the residence time of ophthalmic formulations is using thermosensitive in situ gel. Generally, thermosensitive in situ gel systems are composed of one or more hydrophilic polymers with varying physio-chemical properties. In situ gel-forming systems are mostly fabricated by sodium alginate [15], poloxamer 407 [16], gellan gum [17] and HPMC [18], etc. for glaucoma management has been investigated. These systems showed more stability and exhibit sol-to-gel phase transitions due to a change in a specific physicochemical parameter at environmental conditions on their target sites. In recent years, PCL is a USFDA approved biocompatible polymer and widely employed in biomedical including implants [19], thin films [20] and nanofibers [21] and also for drug delivery for glaucoma [22]. Vitamin E-TPGS is a synthetic, a water-soluble derivative of natural tocopherol and synthesized by esterification of vitamin E succinate with polyethylene glycol (PEG) 1000 [23]. In recent research, TPGS exhibit co-polymerization with various polymers like PLGA [24], PCL [25], and PLA [26] for different drug delivery systems. The PCL-TPGS copolymer has been already explored for various drug delivery systems like cancer chemotherapy [27], schizophrenia [28], hypocalcaemia defect [29], neurodegenerative disorder [30], and fungal infection [31], etc. but not reported for glaucoma management. PCL/vitamin E-TPGS copolymers could be prepared by ring-opening polymerization and simple conjugation method. In the present study, the physical admixture of two different materials (PCL/vitamin E-TPGS) was used for nanoparticles preparation using nanoprecipitation method [32]. The above system undergoes rapid gelation by addition of thermosensitive polymer (Poloxamer) after instilled into cul-de-sac by temperature at 37 °C of eye and provide sustained release of drug [33]. In this study, PCL-TPGS nanoparticles of BRT incorporated into thermosensitive in situ gel systems which provide sustained release as well as enhanced drug permeation and made an important contribution in the clinical phase. In addition, deciphering the role of novel nano-in situ gel for glaucoma was thoroughly characterized by the surface morphology and rheology. In vitro release study, precorneal release study, ocular toxicity, and IOP examination in a rabbit model were also explored to predict its feasibility in overcoming ocular barriers to glaucoma drug delivery.

## 2 Materials and methods

### 2.1 Materials

PCL was purchased from Sigma Aldrich (USA). Poloxamer 407, BRT, and vitamin E TPGS were procured as a gift sample from BASF India Limited (Thane, India), Enaltec (Navi Mumbai, India), and Hetro Pharma (Hyderabad, India), respectively. BRT eye drops i.e., Alphagan Z®, Allergan (India) was purchased from a local pharmacy. All other chemicals used in the study were of analytical grade.

## 2.2 Methods

### 2.2.1 Preparation of nanoparticles

Drug-loaded nanoparticles were prepared using nanoprecipitation method as described previously [34, 35]. Briefly, at room temperature, an organic solution of PCL (0.25–0.4% w/v) in acetone (10 ml) was added to 20 ml of aqueous TPGS solution (0.3–0.5% w/v) and BRT (0.1%) at different stirring speed as shown in Table 1. Nanoparticles dispersion was obtained after solvent evaporation. Then, nanoparticles were separated after centrifugation (Hettich Mikro 220R Centrifuge, UK) of nanoparticles dispersion for 60 min at 16,000 rpm maintained at 4 °C. Pellet of BRT nanoparticles obtained after centrifugation were washed thrice with distilled water. Finally, the developed nanoparticles were lyophilized using freeze drier (Labconco, USA).

### 2.2.2 Characterization of nanoparticles

**2.2.2.1 Particle size, PDI and zeta potential** Two milliliters of preparation were taken in a sample cell and mean particle size, and PDI were determined at room temperature (24 ± 2 °C). All prepared drops were measured in a direction perpendicular to the light scattering angle [36, 37]. Particle size analysis and zeta potential of developed formulation were carried out using a Zetasizer (Malvern Instrument Ltd, UK). To ensure accurate results each observation was carried out in triplicate.

**2.2.2.2 %EE** Percentage of drug encapsulated in nanoparticles was determined by subtracting the unencapsulated amount of drug from total drug concentration (BRT). Five milliliters of BRT-loaded nanodispersion was centrifuged for 1 h at 17,500 rpm at 4 °C (Hettich Mikro 220R Centrifuge, UK). Supernatant was analyzed for drug content using a spectrophotometrically at 246 nm. %EE was calculated by using given below formula.

$$\%\,\text{Encapsulation efficiency} = \frac{W_{\text{total}} - W_{\text{unencapsulated}}}{W_{\text{total}}} \times 100 \quad (1)$$

$W_{\text{total}}$ = amount of drug added to the formulation
$W_{\text{unencapsulated}}$ = amount of unencapsulated drug

**2.2.2.3 Fourier transform infrared spectroscopy (FTIR)** All experiments were recorded at room temperature (25 ± 0.5 °C) and dry conditions. FTIR was used to study the interaction between BRT, excipients, physical mixture, and drug-loaded formulation. FTIR spectroscopy instrument Shimadzu (FTIR 8400S), Japan was used for the study. FTIR spectra of samples were obtained by scanning on spectral range from 4000 to 600 $cm^{-1}$ by using the potassium bromide pellet technique.

**2.2.2.4 Differential scanning calorimetry (DSC)** DSC was performed using differential scanning calorimeter (Perkin-Elmer, USA). To access the interaction between drug and excipients thermograms have been constructed the thermogram using DSC. Thermograms were carried out by heating the sample in an aluminum foil at a rate of 10 °C/min at 25–250 °C [38].

**2.2.2.5 Surface morphology study** Transmission electron microscopy (TEM) of prepared nanoparticles of BRT was performed to analyze the surface morphology. For this study, the nanoparticles were sprinkled onto a glue carbon tape and sputter-covered (Balzer Union SCD040 coater) with gold under vacuum [39]. The pictures were taken utilizing a Carl Zeiss checking electron magnifying instrument at 15 kV.

### 2.2.3 Preparation of BRT-PCL-TPGS nanoparticles loaded in situ gel

Preparation of nanoparticles loaded in situ gel was prepared by the cold method [40]. Briefly, various ranges of poloxamer 407 were kept overnight for 8–10 h in refrigerator (at 2–4 °C). Under magnetic stirring (350 rpm) BRT-PCL-TPGS nanodispersion was added in polymeric solution. Based on gelling capacity and gelling temperature, the formulation was selected for further evaluation [41].

**Table 1** Composition and physicochemical properties of BRT-loaded PCL-TPGS nanodispersion (mean ± SD, $n = 5$)

| Codes | PCL (w/v) | Vitamin E TPGS (w/v) | Speed (rpm) | Particle size (nm) | PDI | Zeta potential (mV) | EE (%) |
|---|---|---|---|---|---|---|---|
| PK-1 | 0.4 | 0.3 | 1200 | 243.40 ± 5.21 | 0.103 ± 0.020 | 3.23 ± 0.01 | 78.87 ± 5.32 |
| PK-2 | 0.25 | 0.4 | 1200 | 255.20 ± 8.51 | 0.140 ± 0.040 | 3.21 ± 0.12 | 71.08 ± 8.35 |
| PK-3 | 0.25 | 0.5 | 1600 | 241.00 ± 7.67 | 0.092 ± 0.050 | 4.85 ± 0.08 | 64.20 ± 6.20 |
| PK-4 | 0.25 | 0.3 | 800 | 276.40 ± 8.61 | 0.159 ± 0.020 | 3.20 ± 0.09 | 72.40 ± 7.54 |
| PK-5 | 0.4 | 0.5 | 1200 | 245.31 ± 10.26 | 0.105 ± 0.040 | 3.75 ± 0.01 | 68.30 ± 5.32 |
| PK-6 | 0.4 | 0.4 | 800 | 318.10 ± 9.27 | 0.245 ± 0.030 | 2.84 ± 0.08 | 81.93 ± 6.61 |

### 2.2.4 Evaluation of BRT-PCL-TPGS nanoparticles loaded in situ gel

**2.2.4.1 Determination of physical appearance and pH** Formulation appearance like clarity and color was determined by visual examination against black and white background before and after gelling. All preparations were tested for pH using pH meter (Hanna Instruments, Romania) in triplicate. The average reading was recorded.

**2.2.4.2 Determination of gelation temperature** Phase transition temperature of the gel was measured as per the method described by [42]. Two milliliters of all formulation were placed in a clear borosilicate glass test tube with gentle stirring and sealed by parafilm. The test tube in an aqueous bath heated at 4 °C with a gradual increase in temperature by 1 °C/min, and allows it to equilibrate for about 15 min until the formulation solution gets gelled. The samples were measured for phase transition, which is considered to have occurred when the bifocal would no longer move when tilted not less than 90°. The measurements of samples were performed in triplicates for accuracy.

**2.2.4.3 Determination of gelation time** It was done by tube inversion method [43]. Briefly, a test tube containing 2 ml of in situ gel of all batches were placed in a water bath kept at 4 °C, adjusted at the gelation temperature i.e., 37 °C. At different intervals of time, sol-to-gel transition was examined for gelation by inverting the test tube. Gelation time was noted in case there was no flow when the test tube was overturned.

**2.2.4.4 Viscosity measurement** Viscosities of PCL-vitamin E TPGS nanoparticles of BRT based in situ were estimated by Rheometer (Rheolab QC, Anton Paar Ltd, Austria) outfitted with a cup and bob type geometry. The estimation of consistency for all tests was performed at the steady shear rate of 100 $s^{-1}$ include the meantime 33 s. The Rheoplus® 32v3.40 programming was utilized for the consistency estimation of gel.

**2.2.4.5 In vitro drug release studies** In vitro study was performed using multi-station (six stages) Franz diffusion assembly (Orchid Scientific, Nashik, India). The permeation study of BRT-PCL-vitamin E TPGS nanoparticles loaded in situ gel was explored utilizing simulated tear fluid (pH 7.4) as the medium and temperature at 37 ± 1 °C. At various time intervals (1, 2, 3, 4, 8, 12, 16, and 24 h) samples were collected and analyzed for drug release by UV-spectrophotometer at 246 nm [44, 45].

**2.2.4.6 Transcorneal ex vivo permeation study** Naturally extracted goat cornea of full-thickness was fixed between donor and acceptor compartments of Franz diffusion using clamped. The corneal area accessible for dispersion was 1.73 $cm^2$. The receptor compartment was loaded up with 7 ml of simulated tear fluid (pH 7.4) and all the air bubbles were removed from the receptor compartment [46]. The receptor liquid was kept at 37 °C using a magnetic bead. About 1 ml of the sample was pulled back from the receptor compartment at different time intervals and was analyzed for BRT content by UV Spectrophotometer. Likewise, marketed preparations of BRT were additionally utilized ($n = 3$) to contemplate transcorneal saturation crosswise over goat cornea to get relative outcomes.

**2.2.4.7 Ocular irritancy test** To verify the safety of an optimized in situ gel study was performed as per OECD guideline 405 (Acute Eye Irritation/Corrosion) [47]. The effectiveness of tested in situ gel was explored by observing the various parameters like redness, frequency of tear production, and corneal ulceration/inflammation after application to rabbit's eyes. In this study, three healthy White New Zealand rabbits (3.5–3.5 kg) were taken. A single dose of 50 µl of in situ was instilled in the lower conjunctival sac of the left eye of animal. Untreated eye used as control. At various time points for 3 days, animals were observed for presence of any ocular defects [48].

**2.2.4.8 Antioxidant studies** 1,1-diphenyl-2-picryl-hydrazyl (DPPH) radical scavenging activity of BRT-PCL-TPGS nanoparticles was analyzed by the previously performed method [49]. Results were expressed in percentage of radical scavenging activity using ascorbic acid as standard. Nanoparticles dispersion (1 ml) was blended with 2 ml of newly prepared solution of DPPH with strength 40 mg/l in methanol and allowed to complete reaction for 30 min. The analysis scavenging activity of DPPH was carried out using a UV-Visible spectrophotometer at λ max of 515 nm [50]. The percentage of radical scavenging activity was estimated by given below formula.

$$\text{Percentage of Radical scavenging activity} = \frac{A_o - A_{\text{sample}}}{A_0} \times 100 \quad (2)$$

$A_0$ = absorbance of control

$A_{\text{sample}}$ = absorbance of samples

**2.2.4.9 IOP study** The glaucoma was induced in White New Zealand experimental rabbits by previously described steroid model [51]. The study was approved by the "Institutional Animal Ethics Committee" (IAEC), DIPSAR, New Delhi (India) with the protocol number (IAEC/2016-I/12). Rabbits were selected (3–3.5 Kg) and divided into three groups.

Group I received marketed formulation and group II was treated with optimized BRT-PCL-TPGS nanoparticles loaded in situ gel and group III was treated as control. Compared the percentage reduction of IOP of rabbits given optimized sol with the marketed eye drop was studied with the help of tonometer (Nidek Non-contact tonometer), at different intervals. A single 50 µl dose of 0.1% BRT loaded in situ gel was instilled onto cornea of animals left eye. At different time intervals, IOP was determined. The right eye was used as a control. Using the following equation, percentage decrease in IOP at many time points were calculated by given below formula [52].

$$\text{Percentage decrease in IOP} = \frac{IOP_{\text{Control}}\ \text{eye} - IOP_{\text{Treated}}\ \text{eye}}{IOP_{\text{Control}}\ \text{eye}}. \quad (3)$$

## 3 Results and discussion

### 3.1 Evaluation of nanoparticles

#### 3.1.1 Particle size, PDI, zeta potential, and % EE

Nanoparticles were prepared batch-wise using various concentrations of PCL and TPGS at different speed. Prepared nanoparticles exhibit size in the range of 241.00–318.10 nm, with a PDI ranging from 0.092 to 0.245 depending on the proportion of PCL and TPGS concentration (Table 1). The mean particle size for optimized BRT-PCL-TPGS nanoparticle (PK-1) was found to be 243.40 ± 5.21 nm and the PDI value was 0.103 ± 0.020 (Fig. 1a). The particle size of BRT-PCL-TPGS nanoparticles were slightly increased with increase of PCL concentration and decreased with increase in stirring speed. Increase in the

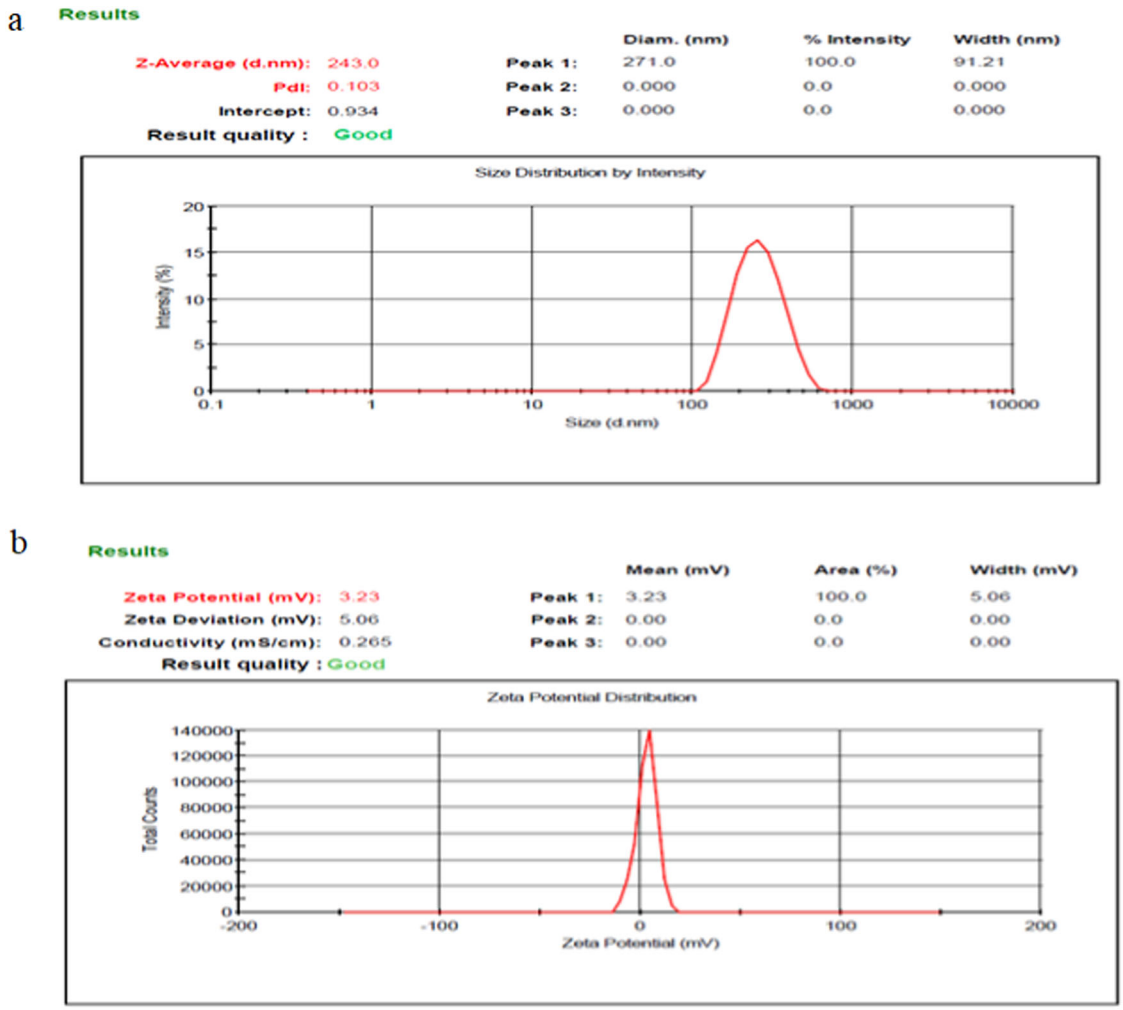


**Fig. 1** **a** Particle size and size distribution (PDI) of optimized nanoparticle and (**b**) zeta potential of optimized nanoparticles

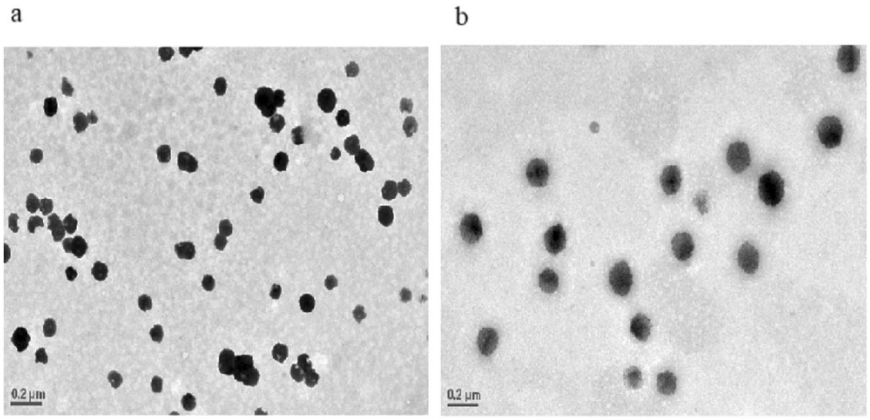


**Fig. 2** TEM images of (**a**) blank PCL-TPGS nanoparticles, and (**b**) optimized BRT loaded PCL-TPGS nanoparticles

concentration of polymer increases the diffusional resistance to BRT molecules from organic phase to the aqueous phase resulting in entrapping more BRT in polymer chains. In fact, the length of diffusional pathways into the aqueous phase increases by the increase in particle size which results in reducing the drug loss through diffusion and increasing BRT amount. Also at higher polymer concentration, the required time for polymer precipitation decreases, so there is less time for diffusion of drug molecules out of nanoparticles, which increases the drug content.

The results indicated that EE decreases with increasing surfactant concentration behind a certain limit. With an increase in surfactant concentration in the external aqueous phase, BRT may diffuse out from the nanodroplets and solubilize as micelles in the aqueous phase. As more BRT molecules solubilize in the external aqueous phase, the amount of surfactant available at the aqueous/organic phase interface decreases and thus agglomeration of nanodroplets may take place [53]. The obtained ranges of particle size were well tolerated and easily permeated by rabbit's eye [54]. Zeta potential of optimized BRT-PCL-TPGS nanoparticle was found to be $+3.23 \pm 0.01$ mV, which portrayed the stability of polymeric nanoparticles (Fig. 1b). The negative charge of outer layer of cornea and mucus layer of tear film can easily interact with positively charged nanoparticles. Therefore, nanoparticles easily permeate through cornea and also prolong retention period on corneal layer. In a nanosized drug delivery system, zeta potential serves as an important indicator for stability of nanodispersion since nanoparticles having higher negative or positive zeta potential exhibit more repulsive forces which results in increased stability of system. TPGS exhibits a very good emulsifying property, which helps in the creation of uniform and small nanoparticles. Surfactants avoid the polymer aggregation and co-dissolve the drug in the organic phase resulting in more drug encapsulation in nanoparticles. Experimental values of %EE of optimized formulation was $78.87 \pm 5.32\%$. The encapsulation efficiency of

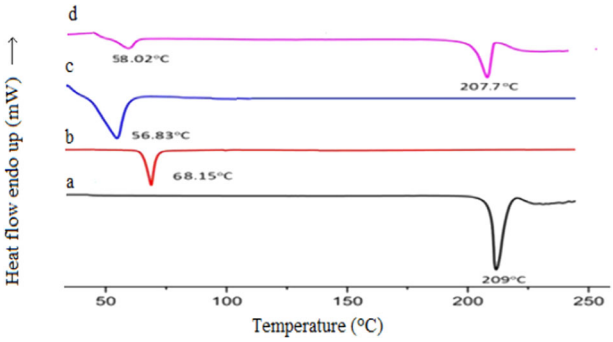


**Fig. 3** DSC thermograms of (**a**) BRT, (**b**) PCL, (**c**) TPGS, and (**d**) optimized nanoparticles

nanoparticles might be increased by the means of more hydrophobicity and lower molecular weight (14 kDa) of PCL as compared with PLGA and PLA copolymer [54, 55].

### 3.1.2 Surface morphology

The morphology of BRT-PCL-TPGS nanoparticles was analyzed by TEM. TEM image for blank PCL is shown in Fig. (2a). BRT-PCL-TPGS nanoparticles are shown in Fig. (2b). BRT-PCL-TPGS nanoparticles exhibited a fairly smooth and spherical morphology. Nanoparticles were discrete, indicating the stability of nanoparticles. Furthermore, nanoparticles exhibited no other colloidal species like drug particles, other than spherical nanoparticles.

### 3.1.3 Differential scanning calorimetry

The scan of BRT-PCL-TPGS was not seen as precisely like the pure drug (Fig. 3). In any case, no significant shift in the endothermic peak was found in physical blends of medication and excipients as contrasted and those of unadulterated medication, which was seen as at 209 °C. In a physical blend of medication and excipients, the top was found at 205.71 °C for the medication. In the thermogram of

**Table 2** Interpretation of FTIR spectra for drug incompatibility

| Materials | Characteristic peak ($cm^{-1}$) |
|---|---|
| BRT | 3204.34 O–H(stretching), 1590.80 NH bending vibrations, 1649.44 C=N and C=C stretching vibrations, 1730 C=O group stretching vibrations, 1300 –CN stretching |
| Vitamin E TPGS | 3738.17 carbonyl band, 2885.20 –CH (stretching), 3738.17 terminal hydroxyl group, 1107 C–O (stretching) |
| PCL | 2945.20 asymmetric $CH_2$, 2869.92 symmetric $CH_2$, 1727.75 carbonyl stretching (C=O), 1293.04 C–O and C–C stretching in crystalline phase, 1240.94 asymmetric COC stretching, 1177.39 COC stretching, 1106.85 C–O and C–C stretching in amorphous phase |
| PCL-TPGS-BRT physical mixture | 3201.9 O–H(stretching), 1690 C=N and C=C (stretching), 2880.20 –CH (stretching), 1150 C–O (stretching) |
| Optimized nanoparticles | 3290.20 C–H stretching vibrations, 1717.75 carbonyl stretching (C=O) |

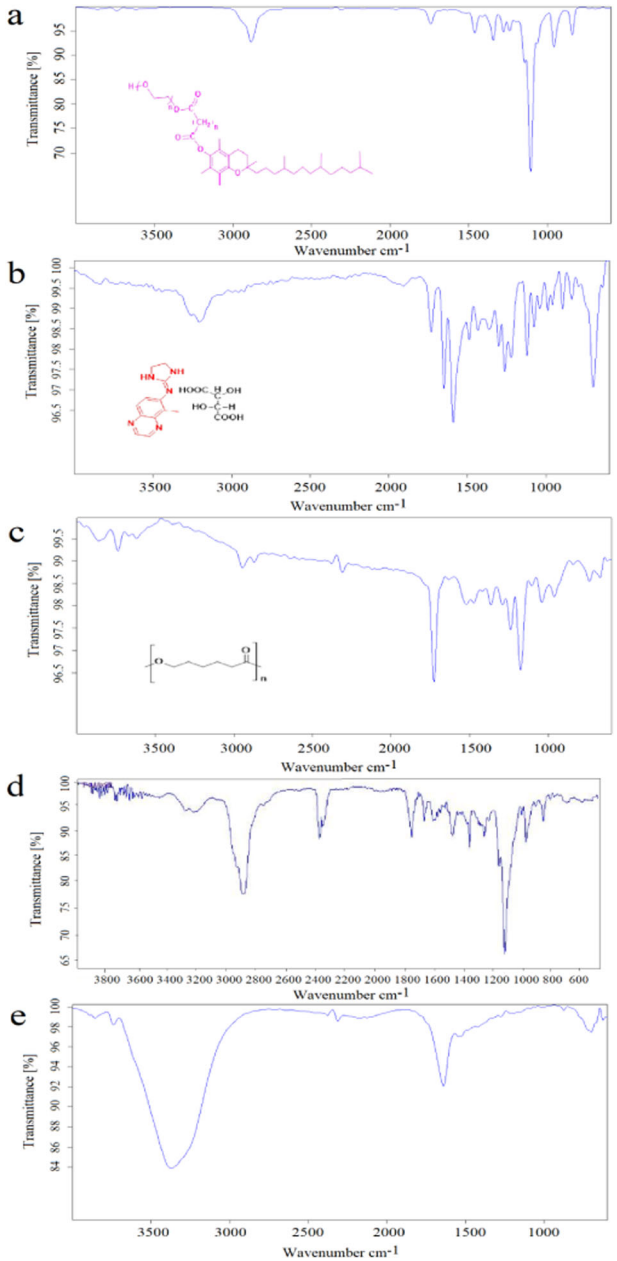


**Fig. 4** FTIR spectra of (**a**) vitamin E TPGS, (**b**) BRT, (**c**) PCL, (**d**) physical mixture, and (**e**) optimized nanoparticles

the upgraded plan, the dissolving endothermic pinnacle showed up close to the softening temperature of BRT and was rough of the same power, henceforth the warm conduct information additionally proposed that the crystallinity of unadulterated BRT has not been decreased in the entangled structure.

### 3.1.4 FTIR

The identity and possible interaction between BRT, vitamin E TPGS, PCL, poloxamer, PCL-TPGS nanoparticles were done with the help of FTIR. The different characteristic peaks of drug, physical mixture, excipients, and formulation are listed in Table 2. FTIR spectra of vitamin E TPGS is shown in Fig. 4(a). The carbonyl band and –CH stretching of TPGS appeared at 1741.47 and 2885.20 $cm^{-1}$, respectively. The absorption band at 3738.17 $cm^{-1}$ was attributed to terminal hydroxyl group and that at 1107 $cm^{-1}$ was due to C–O stretching [56]. In Fig. 4 structure of vitamin TPGS, PCL, and BRT are represented. FTIR spectra of BRT is shown in Fig. 4(b) showing characteristic NH bending vibrations at 1590.80 $cm^{-1}$, C = N, and C = C stretching vibrations at 1649.44 $cm^{-1}$, and the C = O group stretching vibrations at 1730 $cm^{-1}$. There was also –CN stretching at 1300 $cm^{-1}$ [57, 58]. PCL exhibit its characteristic peaks at 2945.20 $cm^{-1}$, 2869.92 $cm^{-1}$, 1727.75 $cm^{-1}$, 1293.04 $cm^{-1}$, 1240.94 $cm^{-1}$ and 1177.39 $cm^{-1}$ were assigned to the asymmetric $CH_2$, symmetric $CH_2$, carbonyl stretching (C = O), C–O and C–C stretching in crystalline phase, asymmetric COC stretching, and COC stretching, respectively as shown in Fig. 4(c). The peaks at 1106.85 $cm^{-1}$ showed the presence of C–O and C–C stretching in amorphous phase [59]. In Fig. 4(d) it was observed that all major peaks in FTIR of the pure drug were retained in the physical mixture of drug, PCL, and vitamin E TPGS suggesting that there was no interaction between BRT and excipients. FTIR spectra of the physical mixtures of BRT with excipients are represented in Fig. 4(d). Showing preservation of the characteristic bands of BRT after mixing, indicating the lack of interference with the

used excipients. The main characteristic peak of BRT structure expressed less intensity in BRT loaded PCL-TPGS nanoparticles and gives an idea about encapsulation of the drug in polymeric nanoparticles [60].

## 3.2 Evaluation of BRT-PCL-TPGS nanoparticles loaded in situ gel

### 3.2.1 Determination of physical appearance and pH

All formulations were clear and colorless but little translucent due to the opalescent nature of nanodispersion. Also, the pH values ranges of 5.8–6.2 which is suitable for ocular application.

### 3.2.2 Determination of phase transition temperature

An increase in the concentration of the polymer, the gelation temperature of gel reduced for all batches. The polyoxyethylene chains present in the thermosensitive polymers (poloxamer) lowers gelation temperature. Increasing the concentration of any of the mucoadhesive polymers used from 12 to 21% produced a gradual decrease in the gelation temperature of the respective solutions [61]. The results of phase transition temperatures of various batches are indicated in Table 3.

### 3.2.3 Determination of gelation time

Preferably, the sol is likely to form gel instantly or in a very short time on exposure to its gelation temperature to avoid rapid elimination by tears. Formulation F-1 take maximum time to gelation, a clear reason for this is less concentration of poloxamer 407, illustrated in Table 3. Formulation F-4 showed a very short gelation time of ~15.66 s, owing to a high percentage of poloxamer 407. Results showed that reduction in sol-gel transition temperature is associated with more poloxamer content accompanied by a short time of gelation [62]. Based on gelling capacity, gelation time, gelling temperature, and viscosity, F-3 formulations were selected for further evaluation.

### 3.2.4 Gelling capacity and viscosity measurement

For improving better flow property, gelling property, and reduced total polymer load, a thermoresponsive in situ gelling polymer and viscosity modifier (poloxamer) as was selected. Various concentrations of Poloxamer-407 were used and characterized for gelling capacity and a viscosity [63]. Formulation (F-1) containing lowest polymer content (i.e., 13% of poloxamer-407), showed low gelling capacity with '*' grade gel, as it remains in sol form at 37 °C. At the hand of all remaining formulations, as increased poloxamer concentration (15–19%) in all formulation batches gelling capacity grades and viscosity were gradually increasing at corresponding physiological temperature (Table 3). From these findings, it can be said that the thermo-responsiveness of poloxamer gel considerably relies on concentration. The higher amount of poloxamer 407 leads to rapid gelation, but at lower gelation temperature. This might be due to the fact, that when the amount of polymers increases, there is increased cross-linking among the adjacent micelles leading to greater viscosity [64].

### 3.2.5 In vitro drug release

From the study findings, it was observed that the in vitro drug release profile of Alphagan Z® (0.1 %) shows a rapid release profile than the optimized BRT- PCL-TPGS nanoparticles loaded in situ gel (Fig. 5). The optimized in situ gel

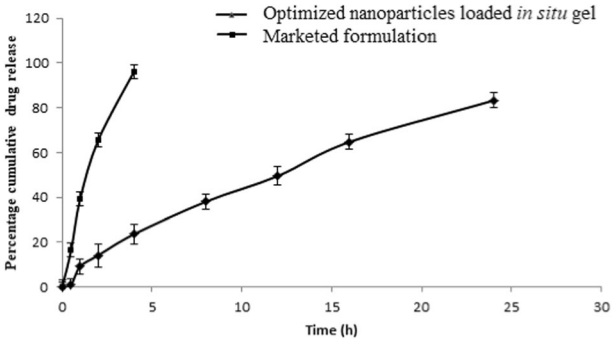


**Fig. 5** Drug release pattern of marketed formulation and optimized nanoparticles loaded in situ gel

**Table 3** Characteristic parameters of BRT nanoparticle-loaded in situ gel

| Formulation | Polaxamer-407 (% w/v) | Gelation time (s) | Gelling capacity | Gelling temperature (°C) | Viscosity (cps) |
|---|---|---|---|---|---|
| F-1 | 12 | 31.55 ± 1.21 | * | 48.12 ± 2.51 | 61.23 ± 9.65 |
| F-2 | 14 | 25.12 ± 0.98 | ** | 40.21 ± 5.21 | 132.25 ± 8.03 |
| F-3 | 17 | 20.98 ± 1.87 | *** | 37.10 ± 0.5 | 713.24 ± 9.19 |
| F-4 | 21 | 15.66 ± 0.22 | **** | 30.25 ± 1.11 | 845.25 ± 12.63 |

*Gelation occurred in few minutes and remained for few hour, **Gelation immediate, remained for few hour, ***Gelation immediate, and for extended period, ****Very stiff gel

**Table 4** In vitro drug release kinetics studies of marketed formulation and optimized in situ gel

| Model name | Zero order | | First order | | Huguchi | | Kor's peppas | | Hix. Crow | |
|---|---|---|---|---|---|---|---|---|---|---|
| | $R^2$ | $K_0$ | $R^2$ | $K_1$ | $R^2$ | $k_H$ | $n$ | $k$ | $R^2$ | $k$ |
| Alphagan Z® eye drop | 0.98 | 0.853 | 0.871 | −0.0304 | 0.930 | 9.87 | 1.95 | 0.136 | 0.9153 | 0.1361 |
| Optimized in situ gel | 0.976 | 0.058 | 0.983 | −0.0012 | 0.922 | 9.10 | 0.942 | 0.942 | 0.9958 | 0.0003 |

**Table 5** Corneal permeation parameter

| Formulation | Steady-state flux J ($\mu g\,cm^{-2}\,h^{-1}$) | Permeability coefficient $P$ ($cm\,h^{-1}$) |
|---|---|---|
| Marketed formulation | 7.618 | 1.5236 |
| BRT-PCL-TPGS nanoparticle based in situ gel | 51.18 | 10.236 |

showed 26.94 ± 3.51% at 4 h and followed by sustained release 93.91 ± 3.12% up to 24 h whereas marketed eye formulation showed at 96.98 ± 2.11% at 2 h. The optimized in situ gel containing poloxamer 407 (17%) exhibited slow and sustained drug release rates were observed. It was explored that in situ gel might be better holding capacity of drug nanoparticles and makes the formulation therapeutically efficient [65]. A rapid release mechanism of in vitro drug release profiles indicates mainly two processes: relocation of water molecules directly into the in situ gel and diffusion of the drug. In vitro drug released data follows mixed release kinetic i.e., zero-order release model ($R^2 >$ 0.98) Higuchi diffusion model ($R^2 > 0.93$) given in Table 4.

The best $R^2$ value of zero-order model was observed for Alphagan Z® drop indicating concentration independent drug release. In the Hixson–Crowell model, good $R^2$ value was observed for optimized in situ gel indicating change in surface area of gel matrix with progressive dissolution of matrix as function of time. These results concur with those of Saindane and associate [66].

### 3.2.6 Transcorneal permeation study

Transcorneal permeation study of optimized in situ gel was compared with the marketed formulation of BRT. The developed in situ gel showed a higher permeation rate through the goat eye 51.18 $\mu g\,cm^{-2}\,h^{-1}$ in 4 h whereas marketed eye drop showed 7.618 $\mu g\,cm^{-2}\,h^{-1}$ transcorneal flux in 4 h (Table 5). The higher permeability coefficient of in situ gel remarks the sustained release with a controlled permeation of 10.23 $P$ ($cm\,h^{-1}$) of the drug from the PCL when compared with the marketed formulation which showed 1.52 $P$ ($cm\,h^{-1}$) permeation [65, 67].

### 3.2.7 Antioxidant studies

DPPH free radical assay is fast and simple screening technique which compares their effectiveness of radical-scavenging activity of samples or formulation with

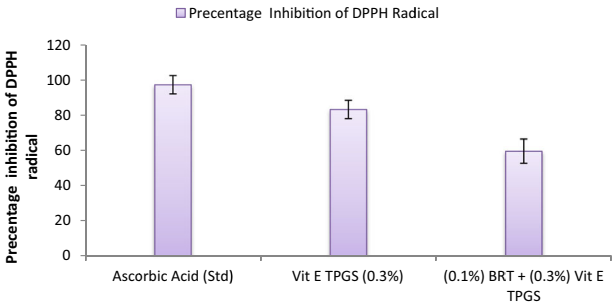


**Fig. 6** DPPH scavenging activity vitamin E TPGS and optimized in situ gel

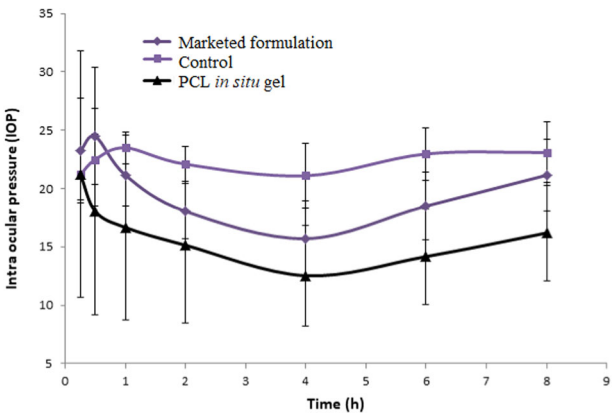


**Fig. 7** IOP activity of marketed formulation and BRT-PCL-TPGS loaded nanoparticles incorporated in situ gel

standard [68]. Vitamin E TPGS composed of d- Tocopherol (27%) and PEG 1000 (65%) and remaining (8%) of succinic acid [69]. In the studies, the free radical-scavenging activity of vitamin E TPGS (0.3%) was 83.21 ± 5.21% which is nearest to standard value of ascorbic acid (97.31 ± 3.23%). The scavenging activity of BRT-PCL-TPGS nanoparticles (59.56 ± 6.84%) was mainly provided by vitamin E TPGS group present in it (Fig. 6).


**Fig. 8** Appearance of rabbit eyes treated with 100 µl of (**a**) marketed eye drop (0.1%), and (**b**) BRT-PCL-TPGS nanoparticles loaded in situ gel

#### 3.2.8 Pharmacodynamic study for the evaluation of IOP

The in vivo IOP results explained that Alphagan Z® showed a decreased IOP reaching its maximum value of 15.7 ± 2.6 at 4 h and then returned to decreasing the normal value of IOP rapidly. The percentage reduction of IOP of BRT-*PCL*-TPGS nanoparticles in situ gel (38.36 ± 3.21%) was higher than marketed formulation (19.5 ± 3.1%) till 6 h. After 6 h, marketed formulation was found to rapidly decreasing its IOP activity, the percent of reducing IOP value close to normal i.e., 9.1 ± 3.3% at 8 h. In addition, novel optimized in situ gel (29.92 ± 2.54) has highest percentage reduction of IOP till 8 h (Fig. 7). Based on these results, two outcomes are observed in this formulation; firstly, in situ gel has mucoadhesive property which adhere to the cornea of eye therefore reduction of drug loss. Secondly, drug nanoparticles easily permeate to corneal surface and reaches to target sites, as a result of which the absorption of BRT has longer period of time for reducing of IOP [70]. It was evident that the nanoparticles loaded in situ gel exhibit a considerable IOP reducing activity for a prolonged period of time as compared with that of a marketed eye drop. Nanoparticles loaded in situ gel enhances up-take favorably by modifying the drug release characteristics of drug through the cornea.

#### 3.2.9 Ocular irritancy test

The eye irritation studies as a result of in situ gel administration into the left eye of albino rats were evaluated for next 3 days. The formulation was graded for eye lesions, and no ocular damage was observed into the cornea, iris of the eye (Fig. 8). Therefore, the optimized formulation incorporated into in situ gel was found to be safe, non-irritant and non-corrosive.

## 4 Conclusion

BRT loaded PCL-TPGS nanoparticles were developed using PCL and vitamin E TPGS using nanoprecipitation technique. In addition, the study also explored the inclusion of the nanodispersion into poloxamer 407 based thermosensitive in situ gel for ocular management. The formulation was in sol form at room temperature and underwent rapid gelation upon raising temperature to 37.10 ± 0.5 °C. The ratio of PCL-vitamin E TPGS (1:1.25) nanodispersion exhibited small particles size and high EE. PK-1 formulation was therefore selected to be incorporated into poloxamer (17%) based thermosensitive in situ gel. In situ (F3) was selected on the basis of good quality of gelling capacity, gelling time, and viscosity. The results of in vitro and transcorneal permeation release studies confirmed the sustained release of drug from prepared in situ gel up to 24 h. In DPPH assay, the studies showed that optimized in situ gel showed free radical-scavenging activity as compared with ascorbic acid as standard. Nanoparticles loaded in situ gel showed better IOP lowering capacity as compared with marketed eye drops till 8 h. After application of prepared gel in eyes no ocular irritancy was observed. The ex vivo permeation study showed that the prepared formulation BRT-PCL-TPGS permeated greater amount of drug per unit of time than other formulation tested justifying that the nanoparticles had a greater IOP reducing effect to the commercial formulation in the in vivo study. The developed nanoparticles loaded in situ gel may confirm to be a good alternative to conventional formulations, and could be utilized in the management of glaucoma. These nanoparticulate drug delivery in situ gel system exhibited better ocular drug efficacy by improving ocular bioavailability without blurring the vision in glaucoma, thus increasing the patient compliance.

## Compliance with ethical standards

**Conflict of interest** The authors declare that they have no conflict of interest.

**Publisher's note** Springer Nature remains neutral with regard to jurisdictional claims in published maps and institutional affiliations.

## References


1. Abdelrahman AM (2015) Noninvasive glaucoma procedures: current options and future innovations. Middle East Afr J Ophthalmol 22:2–9
2. Bachu RD, Chowdhury P, Al-Saedi ZH, Karla PK, Boddu SH (2018) Ocular drug delivery barriers—role of nanocarriers in the treatment of anterior segment ocular diseases. Pharm Dev Tech 16:627–636
3. Sutradhar KB, Amin ML (2013) Nanoemulsions: increasing possibilities in drug delivery. Eur J Nanomed 5:97–110
4. Baranowski P, Karolewicz B, Gajda M, Pluta J (2014) Ophthalmic drug dosage forms: characterisation and research methods. The Sci World J 2014:1–14
5. Agarwal R, Iezhitsa I, Agarwal P, Abdul Nasir NA, Razali N, Alyautdin R, Ismail NM (2016) Liposomes in topical ophthalmic drug delivery: an update. Drug deliv 23:1075–1091
6. Fetih G (2016) Fluconazole-loaded niosomal gels as a topical ocular drug delivery system for corneal fungal infections. J Drug Deliv Sci Tech 35:8–15
7. Das S, Suresh PK, Desmukh R (2010) Design of Eudragit RL 100 nanoparticles by nanoprecipitation method for ocular drug delivery. Nanomed: Nanotechnol, Biol Med 6:318–323
8. Ding D, Kundukad B, Somasundar A, Vijayan S, Khan SA, Doyle PS (2018) Design of mucoadhesive PLGA microparticles for ocular drug delivery. ACS Appl Bio Mater 16:561–571
9. Mahmoud AA, El-Feky GS, Kamel R, Awad GE (2011) Chitosan/sulfobutylether-β-cyclodextrin nanoparticles as a potential approach for ocular drug delivery. Int J Pharm 413:229–236
10. Chiang B, Kim YC, Doty AC, Grossniklaus HE, Schwendeman SP, Prausnitz MR (2016) Sustained reduction of intraocular pressure by supraciliary delivery of brimonidine-loaded poly (lactic acid) microspheres for the treatment of glaucoma. J Cont Release 228:48–57
11. Gratieri T, Gelfuso GM, Rocha EM, Sarmento VH, de Freitas O, Lopez RF (2010) A poloxamer/chitosan in situ forming gel with prolonged retention time for ocular delivery. Euro J Pharm and Biopharm 75:186–193
12. Gajrå B, Pandya SS, Vidyasagar G, Rabari H, Dedania RR, Rao S (2012) Poly vinyl alcohol hydrogel and its pharmaceutical and biomedical applications: a review. Int J of Pharm Res 4:20–26
13. Makadia HK, Siegel SJ (2011) Poly lactic-co-glycolic acid (PLGA) as biodegradable controlled drug delivery carrier. Polymers 3:1377–1397
14. Reed K, Berger N (2018) The effect of polyvinylpyrrolidone (PVP) on ocular gel forming solutions composed of gellan and calcium gluconate. Int J Pharm Sci and Res 9:20–28
15. Mandal S, Thimmasetty MK, Prabhushankar GL, Geetha MS (2012) Formulation and evaluation of an in situ gel-forming ophthalmic formulation of moxifloxacin hydrochloride. Int J Pharm Investig 2:78–82
16. Edsman K, Carlfors J, Petersson R (1998) Rheological evaluation of poloxamer as an in situ gel for ophthalmic use. Euro J Pharm Sci 6:105–112
17. Duan Y, Cai X, Du H, Zhai G (2015) Novel in situ gel systems based on P123/TPGS mixed micelles and gellan gum for ophthalmic delivery of curcumin. Colloid Surface B 128:322–330
18. Morsi N, Ibrahim M, Refai H, El Sorogy H (2017) Nanoemulsion-based electrolyte triggered in situ gel for ocular delivery of acetazolamide. Euro J Pharm Sci 104:302–314
19. Pehlivan SB, Yavuz B, Çalamak S, Ulubayram K, Kaffashi A, Vural I, Çakmak HB, Durgun ME, Denkbaş EB, Ünlü N (2015) Preparation and in vitro/in vivo evaluation of cyclosporin a-loaded nanodecorated ocular implants for subconjunctival application. J Pharm Sci 104:1709–1720
20. Bernards DA, Bhisitkul RB, Wynn P, Steedman MR, Lee OT, Wong F, Thoongsuwan S, Desai TA (2013) Ocular biocompatibility and structural integrity of micro-and nanostructured poly (caprolactone) films. J Ocul Pharmacol and Ther 29:249–257
21. Da Silva GR, Lima TH, Oréfice RL, Fernandes-Cunha GM, Silva-Cunha A, Zhao M, Behar-Cohen F (2015) In vitro and in vivo ocular biocompatibility of electrospun poly (ε-caprolactone) nanofibers. Euro J Pharm Sci 73:9–19
22. Nasr FH, Khoee S, Dehghan MM, Chaleshtori SS, Shafiee A (2016) Preparation and evaluation of contact lenses embedded with polycaprolactone-based nanoparticles for ocular drug delivery. Biomacromol 17:485–495
23. Kong LY, Su BG, Bao ZB, Xing HB, Yang YW, Ren QL (2011) Direct quantification of mono-and di-d-α-tocopherol polyethylene glycol 1000 succinate by high performance liquid chromatography. J Chromatogr A 48:8664–8671
24. Alkholief M, Albasit H, Alhowyan A, Alshehri S, Raish M, Kalam MA, Alshamsan A (2019) Employing a PLGA-TPGS based nanoparticle to improve the ocular delivery of Acyclovir. Saudi Pharm J 27:293–302
25. Ren F, Jing Q, Cui J, Shen Y (2009) Synthesis and Characterization of D-α-Tocopheryl Polyethylene Glycol 1000 Succinate-Block-Poly (ε-caprolactone) Copolymer Used as Carriers for Microparticles. J Disper Sci Tech 30:1129–1134
26. Thu HP, Nam NH, Quang BT, Son HA, Toan NL, Quang DT (2015) In vitro and in vivo targeting effect of folate decorated paclitaxel loaded PLA–TPGS nanoparticles. Saudi Pharma J 23:683–688
27. Bernabeu E, Helguera G, Legaspi MJ, Gonzalez L, Hocht C, Taira C, Chiappetta DA (2014) Paclitaxel-loaded PCL–TPGS nanoparticles: In vitro and in vivo performance compared with Abraxane®. Colloid Surface B 113:43–50
28. Zhen L, Wei Q, Wang Q, Zhang H, Adu-Frimpong M, Kesse Firempong C, Xu X, Yu J (2020) Preparation and in vitro/in vivo evaluation of 6-Gingerol TPGS/PEG-PCL polymeric micelles. Pharm Dev Tech 25:1–8
29. Koulouktsi C, Nanaki S, Barmpalexis P, Kostoglou M, Bikiaris D (2019) Preparation and characterization of Alendronate depot microspheres based on novel poly (-ε-caprolactone)/Vitamin E TPGS copolymers. Int J Pharm X 1:100014
30. Zhang Z, Tan S, Feng SS (2012) Vitamin E TPGS as a molecular biomaterial for drug delivery. Biomaterials 33:4889–4906
31. Tang X, Jiao R, Xie C, Xu L, Huo Z, Dai J, Qian Y, Xu W, Hou W, Wang J, Liang Y (2015) Improved antifungal activity of amphotericin B-loaded TPGS-b-(PCL-ran-PGA) nanoparticles. Int J Clin Exp Med 8:5150–5162
32. Mishra B, Padaliya R, Patel RR (2017) Exemestane encapsulated vitamin E-TPGS–polymeric nanoparticles: preparation, optimization, characterization, and in vitro cytotoxicity assessment. Artif Cells Nanomed Biotechnol 45:522–534
33. Almeida H, Amaral MH, Lobão P, Sousa Lobo JM (2013) Applications of poloxamers in ophthalmic pharmaceutical formulations: an overview. Expert Opin Drug Deliv 10:1223–1237
34. Miladi K, Sfar S, Fessi H, Elaissari A (2016) Nanoprecipitation Process: From particle preparation to in vivo applications. In: Vauthier C., Ponchel G. (eds), Polymer Nanoparticles for Nanomedicines. Springer, Cham
35. Bernabeu E, Chiappetta DA (2013) Vitamin E TPGS used as emulsifier in the preparation of nanoparticulate systems. J Biomater Tiss Eng 3:122–134
36. Kumar S, Ali J, Baboota S (2016) Design Expert® supported optimization and predictive analysis of selegiline nanoemulsion via the olfactory region with enhanced behavioural performance in Parkinson's disease. Nanotechnology 27:435101
37. Gupta BK, Kumar S, Kaur H, Ali J, Baboota S (2018) Attenuation of oxidative damage by coenzyme Q10 loaded nanoemulsion

through oral route for the management of Parkinson's disease. Rejuvenation Res 21:232–248
38. Chauhan MK, Sharma PK (2019) Optimization and characterization of rivastigmine nanolipid carrier loaded transdermal patches for the treatment of dementia. Chem Phys Lipids 224:104794
39. Kumar S, Gupta SK (2014) Effect of excipients on dissolution enhancement of aceclofenac solid dispersions studied using response surface methodology: a technical note. Archives Pharmacal Res 37:340–351
40. Lou J, Hu W, Tian R, Zhang H, Jia Y, Zhang J, Zhang L (2014) Optimization and evaluation of a thermoresponsive ophthalmic in situ gel containing curcumin-loaded albumin nanoparticles. Int J Nanomed 9:2517–2525
41. Morsi N, Ghorab D, Refai H, Teba H (2016) Ketoroloac tromethamine loaded nanodispersion incorporated into thermosensitive in situ gel for prolonged ocular delivery. Int J Pharm 506:57–67
42. Hanlon TJ, Coath JA, Richardson MA (2003) Molybdenum-doped vanadium dioxide coatings on glass produced by the aqueous sol–gel method. Thin Solid Films 436:269–272
43. Ur-Rehman T, Tavelin S, Gröbner G (2011) Chitosan in situ gelation for improved drug loading and retention in poloxamer 407 gels. Int J Pharm 409:19–29
44. Kaur IP, Singh M, Kanwar M (2000) Formulation and evaluation of ophthalmic preparations of acetazolamide. Int J Pharm 199:119–127
45. Tayel SA, El-Nabarawi MA, Tadros MI, Abd-Elsalam WH (2013) Promising ion-sensitive in situ ocular nanoemulsion gels of terbinafine hydrochloride: design, in vitro characterization and in vivo estimation of the ocular irritation and drug pharmacokinetics in the aqueous humor of rabbits. Int J Pharm 443:293–305
46. Pathak MK, Chhabra G, Pathak K (2013) Design and development of a novel pH triggered nanoemulsified in-situ ophthalmic gel of fluconazole: ex-vivo transcorneal permeation, corneal toxicity and irritation testing. Drug Dev Ind Pharm 39:780–790
47. Staff OECD (2002) OECD guidelines for the testing of chemicals. Fourteenth addendum Paris OECD Publishing, 1–87. https://www.oecd.org/env/ehs/testing/oecdguidelinesforthetestingofchemicals.htm
48. Kakkar S, Kaur IP (2011) Spanlastics—A novel nanovesicular carrier system for ocular delivery. Int J Pharma 413:202–210
49. Xin J, Tang J, Bu M, Sun Y, Wang X, Wu L, Liu H (2016) A novel eye drop of alpha tocopherol to prevent ocular oxidant damage: improve the stability and ocular efficacy. Drug Dev Ind Pharm 42:525–534
50. Shrotriya S, Ranpise N, Satpute P, Vidhate B (2018) Skin targeting of curcumin solid lipid nanoparticles-engrossed topical gel for the treatment of pigmentation and irritant contact dermatitis. Artificial Cells, Nanomed Biotech 46:1471–1482
51. Gupta SK, Agarwal R, Galpalli ND, Srivastava S, Agrawal SS, Saxena R (2007) Comparative efficacy of pilocarpine, timolol and latanoprost in experimental models of glaucoma. Find Exp Clin Pharmacol 29:665–672
52. Wang F, Chen L, Jiang S, He J, Zhang X, Peng J, Xu Q, Li R (2014) Optimization of methazolamide-loaded solid lipid nanoparticles for ophthalmic delivery using Box–Behnken design. J Lipo Res 24:171–181
53. Baghbani F, Moztarzadeh F, Mohandesi JA, Yazdian F, Mokhtari-Dizaji M, Hamedi S (2016) Formulation design, preparation and characterization of multifunctional alginate stabilized nanodroplets. Int J Biol Macromol 89:550–558
54. Janagam DR, Wu L, Lowe TL (2017) Nanoparticles for drug delivery to the anterior segment of the eye. Adv Drug Deliv Rev 122:31–64
55. Hu C, Chen Z, Wu S, Han Y, Wang H, Sun H, Kong D, Leng X, Wang C, Zhang L, Zhu D (2017) Micelle or polymersome formation by PCL-PEG-PCL copolymers as drug delivery systems. Chinese Chem Lett 28:1905–1909
56. Ren F, Jing Q, Cui J, Shen Y (2009) Synthesis and Characterization of D-α-Tocopheryl Polyethylene Glycol 1000 Succinate-Block-Poly (ε-caprolactone) Copolymer Used as Carriers for Microparticles. J Disper Sci Technol 30:1129–1134
57. Eldeeb AE, Salah S, Ghorab M (2019) Proniosomal gel-derived niosomes: an approach to sustain and improve the ocular delivery of brimonidine tartrate; formulation, in-vitro characterization, and in-vivo pharmacodynamic study. Drug Delivery 26:509–521
58. Aburahma MH, Mahmoud AA (2011) Biodegradable ocular inserts for sustained delivery of brimonidine tartarate: preparation and in vitro/in vivo evaluation. AAPS PharmSciTech 12:1335–1347
59. Elzein T, Nasser-Eddine M, Delaite C, Bistac S, Dumas P (2004) FTIR study of polycaprolactone chain organization at interfaces. J Colloid Interface Sci 273:381–387
60. Zhang Y, Cun D, Kong X, Fang L (2014) Design and evaluation of a novel transdermal patch containing diclofenac and teriflunomide for rheumatoid arthritis therapy. Asian J Pharm Sci 9:251–259
61. Choi HG, Jung JH, Ryu JM, Yoon SJ, Oh YK, Kim CK (1998) Development of in situ-gelling and mucoadhesive acetaminophen liquid suppository. Int J Pharm 165:33–44
62. Ricci EJ, Bentley MV, Farah M, Bretas RE, Marchetti JM. Rheological characterization of Poloxamer 407 lidocaine hydrochloride gels. Euro J Pharm Sci 17:161–167
63. Shin SC, Kim JY, Oh IJ (2000) Mucoadhesive and physicochemical characterization of carbopol-poloxamer gels containing triamcinolone acetonide. Drug Dev Ind Pharma 26:307–312
64. Moebus K, Siepmann J, Bodmeier R (2009) Alginate–poloxamer microparticles for controlled drug delivery to mucosal tissue. Euro J Pharm Biopharm 72:42–53
65. Hao J, Zhao J, Zhang S, Tong T, Zhuang Q, Jin K, Chen W, Tang H (2016) Fabrication of an ionic-sensitive in situ gel loaded with resveratrol nanosuspensions intended for direct nose-to-brain delivery. Colloids Surfaces B 147:376–386
66. Saindane NS, Pagar KP, Vavia PR (2013) Nanosuspension based in situ gelling nasal spray of carvedilol: development, in vitro and in vivo characterization. AAPS PharmSciTech 14:189–199
67. Gratieri T, Gelfuso GM, de Freitas O, Rocha EM, Lopez RF (2011) Enhancing and sustaining the topical ocular delivery of fluconazole using chitosan solution and poloxamer/chitosan in situ forming gel. Euro J Pharm Biopharm 79:320–327
68. Kumar S, Dang S, Nigam K, Ali J, Baboota S (2018) Selegiline nanoformulation in attenuation of oxidative stress and upregulation of dopamine in the brain for the treatment of Parkinson's disease. Rejuvenation Res.1 21:464–476
69. Sokol RJ, Heubi JE, Butler-Simon N, McClung HJ, Lilly JR, Silverman A (1987) Treatment of vitamin E deficiency during chronic childhood cholestasis with oral d-α-tocopheryl polyethylene glycol-1000 succinate. Gastroenterology 93:975–985
70. Gupta S, Samanta MK, Raichur AM (2010) Dual-drug delivery system based on in situ gel-forming nanosuspension of forskolin to enhance antiglaucoma efficacy. AAPS Pharmscitech 11:322–335